2016 American Control Conference (ACC)
Boston Marriott Copley Place
July 6-8, 2016. Boston, MA, USA

Multi-Physics Modeling of Hysteresis in Vanadium Dioxide Thin Films

Chandika Annasiwatta[1], Jinhao Chen[1], Jordan M. Berg[1], Ayrton Bernussi[2], Zhaoyang Fan[2] and Beibei Ren[1]

***Abstract*— Vanadium dioxide (VO_2) exhibits a strong metal-insulator transition (MIT) near 68°C. The resulting changes in electrical, optical, thermal and mechanical properties make VO_2 thin films interesting for a variety of sensor and actuator applications. The transition displays significant hysteresis that may significantly affect device performance. An accurate model of the transition would be valuable for predicting and compensating these effects. In this paper we investigate first-principles, multi-physics models using simultaneous measurement of optical and electrical properties. Our experimental results strongly validate use of a standard Preisach model to capture hysteresis in the optical properties of the VO_2 film. We then investigate several physics-based models relating electrical resistivity to the fraction of material transformed. Of the models investigated, a percolation-based approach is the most successful. There are opportunities for further refinement of the resistivity model and explicit treatment of temperature dependence.**

I. Introduction

Vanadium dioxide (VO_2) exhibits a thermally induced metal-insulator transition (MIT) near 68°C [1]. Below the threshold, the material behaves as a semiconductor. It has a high electrical resistivity, and it is relatively transparent to infrared (IR) light. Above the threshold, the material behaves as a metal. It has a low electrical resistivity, and it becomes a good reflector in the IR. Although the magnitude, sharpness, and center temperature of the transition depend on material composition and micro-structure [3]-[4], electrical resistivity can decrease as much as four orders of magnitude over a temperature increase of 60°C. The transition may also be triggered by electrical or optical inputs [2]. This high sensitivity to temperature makes VO_2 extremely useful for sensing, for example in devices such as IR bolometers and radiation detectors [5]. Changes in optical, mechanical, and thermal properties of VO_2 due to the MIT have also been used as the basis for novel actuator designs, including micro-grippers [6], light modulators [7], and thermal switches [8].

Figs. 1 and 2 show the significant hysteresis typical of optical transmittance and electrical resistance of VO_2 thin films as a function of temperature. This hysteresis makes precise control of the MIT problematic. As a result, most VO_2 applications avoid operating in the transition region. Some model-based approaches have been proposed to suppress hysteretic behavior [9]-[10]. However, improved hysteresis models would improve the ability of device designers to predict material response in high-fidelity simulations, and to compensate the nonlinearity in order to achieve desired dynamic behavior.

Approaches to modeling hysteresis include the Preisach model [11]-[12], the Prandtl-Ishlinskii model [12]-[13], the Duhem model [12], and others [14]-[15]. The intuition underlying the Preisach model is that the material is made of a large number of small domains, each of which behaves as an ideal relay, or *hysteron*, with distinct increasing and decreasing transition values. The Preisach model represents a general hysteresis operator as a linear combination over all such hysterons [11]. For the Preisach model to describe a particular hysteretic behavior, two necessary and sufficient conditions must be satisfied, known as the *wiping-out property* and the *congruency property* [11]. De Almeida et al. observed that the congruency property is not satisfied for hysteresis in the resistance-temperature (R-T) characteristic of VO_2 [16]. To obtain reasonable accuracy from the Preisach model, they considered instead the *logarithm of resistance* versus temperature. Fig. 3 shows a typical $\log R$-T curve.

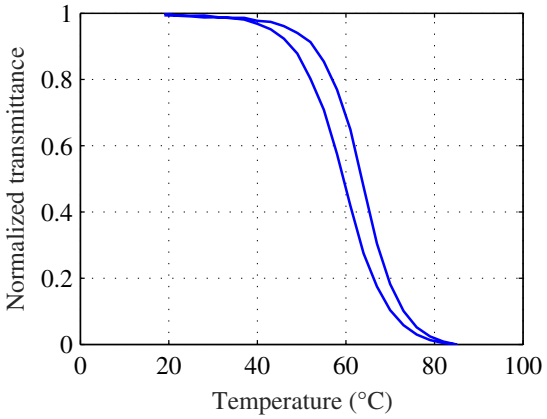

Fig. 1. Transmittance versus temperature for a VO_2 thin film.

In this paper we report experiments that simultaneously characterize the electrical and optical transition in VO_2 films. The electrical measurements confirm the "non-Preisach" behavior reported in [16], ruling out use of an unmodified Preisach model. However the simultaneous optical measurements show that the wiping-out and congruency properties are both satisfied, suggesting that a standard Preisach model will accurately capture the optical hysteresis. One pragmatic

[1] Chandika Annasiwatta, Jinhao Chen, Jordan. M. Berg and Beibei Ren are with the Department of Mechanical Engineering, Texas Tech University, Lubbock, TX, 79409, USA. chandika.annasiwatta@ttu.edu, jinhao.chen@ttu.edu, jordan.berg@ttu.edu, beibei.ren@ttu.edu

[2] Ayrton Bernussi and Zhaoyang Fan are with the Department of Electrical and Computer Engineering, Texas Tech University, Lubbock, TX, 79409, USA ayrton.bernussi@ttu.edu, zhaoyang.fan@ttu.edu

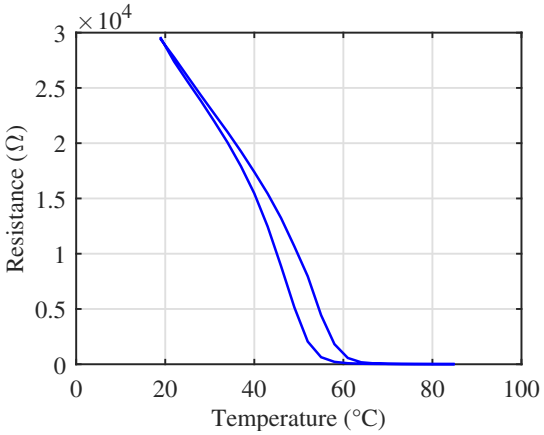

Fig. 2. Resistance versus temperature for a VO_2 thin film.

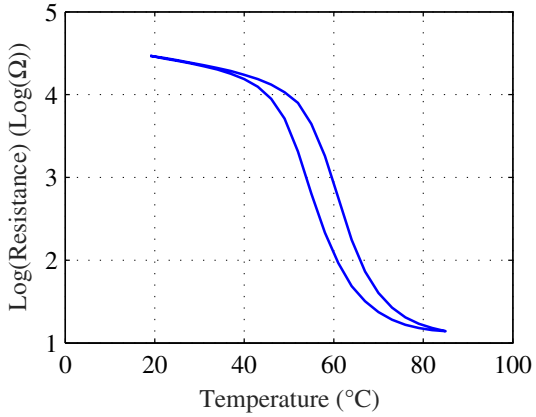

Fig. 3. Logarithm of resistance versus temperature for a VO_2 thin film.

approach to treating the divergent optical and electrical behaviors is simply to derive and use an independent model for each property. In contrast, the object of this paper is to show how an integrated multi-physics model may obtain the observed electrical and optical properties as physically plausible consequences of a single material transition.

Fig. 4 shows the underlying physical intuition. A thin VO_2 film deposited on a substrate is composed of many domains, possibly corresponding to physical grains. Electrical and optical properties are assumed to be uniform within each domain. Optical transmissivity is measured by passing light through the film in the direction normal to the surface. Electrical resistivity is measured by passing current within the film, parallel to the surface. That is, each ray of light in the optical measurement passes through a single domain, while each current streamline in the electrical measurement passes through many domains. To see the consequences of these different measurement geometries, consider the case shown schematically in Fig. 4, and assume that the lighter domains are electrically insulating and optically transparent, while the darker domains are electrically conductive and optically reflective. In Fig. 4(a), approximately 20% of the material has transformed. This change corresponds directly to a 20% drop in transmissivity, since each domain is now either transparent or reflective. However, the transformed film is still an electrical insulator, since the electrically conducting domains are isolated from each other, and there is no contiguous path from edge to edge. In Fig. 4(b), about 60% of the material has transformed. Again, the optical change in transmissivity follows the fraction transformed directly. Now, however, the transformed domains form conductive pathways across the surface, and the electrical resistivity will show a sharp drop.

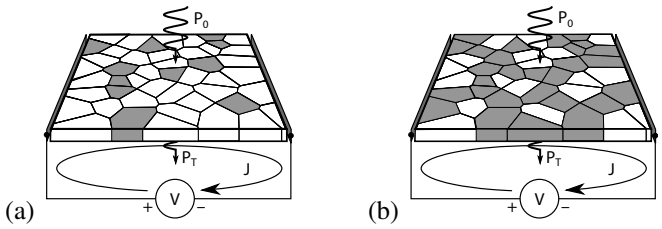

Fig. 4. Schematic of transition in a thin film, with (a) $\sim$ 20% fraction transformed, and (b) $\sim$ 60% fraction transformed. Transformed domains are shaded darker. Optical transmissivity is the ratio P_T/P_0 of transmitted optical power to incident optical power normal to the surface. Electrical resistance, V/J, is measured edge to edge through a square region of the film.

The rest of the paper is organized as follows. Section II describes the apparatus and experimental procedures used to obtain simultaneous optical (P-T) and electrical (R-T) data. Section III discusses modeling of the optical characteristic, and presents results in support of using a standard Preisach model for this purpose. Section IV focuses on deriving the relationship between optical and electrical properties by applying effective medium approximations and percolation models. Finally, Section V presents conclusions from the paper, and future extensions of this work.

II. Experimental Procedure

A 150 nm thick VO_2 film was grown on an a-plane sapphire substrate by reactive DC magnetron sputtering of a 99.95% vanadium metal target in ambient Ar/O_2. The total gas mixture pressure was kept constant at 3 mTorr, with an O_2/Ar flow ratio of 11%. The sample was grown with a substrate heater temperature of 575°C. The substrate was located 8 mm from the resistive heater. After growth, the sample was cooled to ambient temperature in vacuum. Four symmetric Ti/Au contacts were deposited onto the corners of each VO_2 sample using standard photolithography, deposition, and lift-off. These contacts serve as the four probes for resistivity measurements.

Fig. 5 shows the experimental setup. The VO_2 film and sapphire substrate are mounted on a thin aluminum sample holder, which is connected to a large aluminum thermal mass through an electrothermal peltier effect heater/cooler. A lens system directs the output of a 1560 nm infrared laser through a 1% beam splitter and through the VO_2 film. Measurements of the split input beam and the light transmitted through the film and substrate are used to compute the film transmissivity. Simultaneous voltage and current measurements are made to

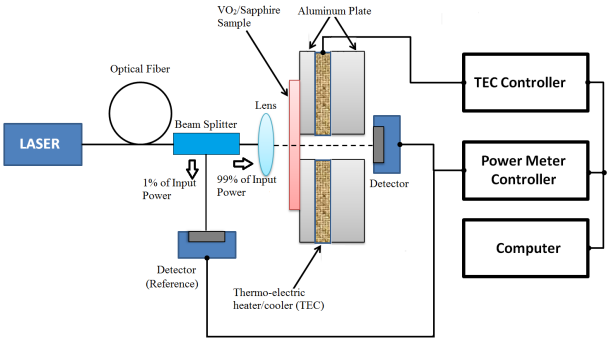

Fig. 5. Experimental setup.

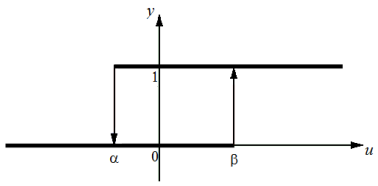

Fig. 6. The relay hysteron.

measure film resistivity using the van der Pauw method [17]. Film properties are characterized from 19°C to 85°C. The large aluminum thermal mass is maintained near 55°C using a simple proportional controller driving a heater element and cooling fan.

III. Hysteresis of Optical Transmittance

The intuitive idea behind the Preisach model is of a small domain of material, such as a single grain, that can exist in one of two states. The state transitions of this domain are assumed to be described by an ideal relay operator, characterized by thresholds α and β. The overall behavior of the system is assumed to be determined by the fraction of material corresponding to each α-β pair. If transition in the domains depicted in Fig. 4 follows such an ideal element, then the overall optical behavior of a thin film should be well described by the Preisach model.

A. Preisach Hysteresis

The relay hysteron $R_{\alpha,\beta}$ shown in Fig. 6 forms the fundamental building block of the Preisach model. The output of $R_{\alpha,\beta}$ depends on its previous state. Mathematically, the output of the relay operator is

$$y(u) = \begin{cases} 1 & u \geq \beta \\ 0 & u \leq \alpha \\ k & \alpha < u < \beta \end{cases} \tag{1}$$

where u is the input, y is the output, α and β are thresholds. k can take either 0 or 1 depending on the previous output. The classical Preisach model is then

$$\hat{\Gamma}[u](t) = \iint_{\beta \geq \alpha} \mu(\alpha, \beta) R_{\alpha,\beta} \, d\alpha \, d\beta \tag{2}$$

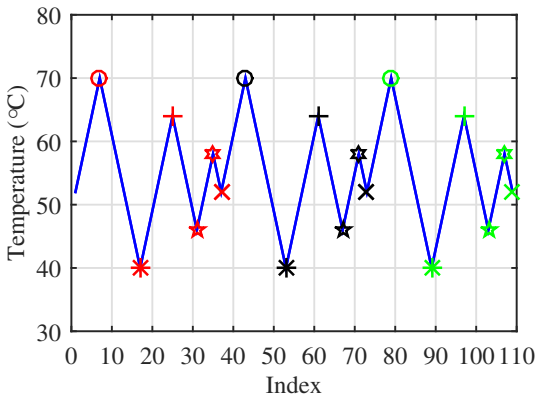

Fig. 7. Temperature profile for validation of the wiping-out property.

where $\hat{\Gamma}$ denotes the Preisach operator. The argument of the operator is written in square brackets to indicate that the output depends on the entire input function, rather than its value at a single point.

Choosing only discrete values α_i and β_j yields a discretized version of the Preisach model. One can visualize the discrete version as a system of relay hysterons connected in parallel, with the net output formed as the weighted sum of the individual outputs. The weights can now be represented as a matrix with $\mu_{ij} \triangleq \mu(\alpha_i, \beta_j)$.

B. Optical Hysteresis Model

The wiping-out and congruency properties are necessary and sufficient for hysteresis to be characterized by the Preisach model [11]. We have experimentally verified both the wiping-out and congruency properties for the P-T characteristic. The wiping-out property is verified using the piecewise monotonic temperature profile as shown in Fig. 7, where different colors are used to indicate repeated occurrence of local temperature maxima and minima. According to the wiping-out property, local maxima and minima marked by the same shapes should be coincident in the P-T curve. From Fig. 8, we observe those points marked by the same shapes are indeed closely matched and coincident. We have experimentally verified the congruency property for the P-T curve, using the following visualization. Consider two minor loops formed between the same two consecutive extrema. Shift the end points to lie on top of each other. If the shifted minor loops are coincident, then they are congruent. The experimental results shown in Figs. 9 and 10 support validity of the congruency property.

Finally, we experimentally identify the Preisach weights for the sample film using the temperature profile shown in Fig. 11. This profile gives a unique set of discrete weights. A random temperature profile is then chosen as shown in Fig. 12 to validate the identified model under a different excitation. Figs. 13 and 14 show that the identified Preisach model matches the validation data well.

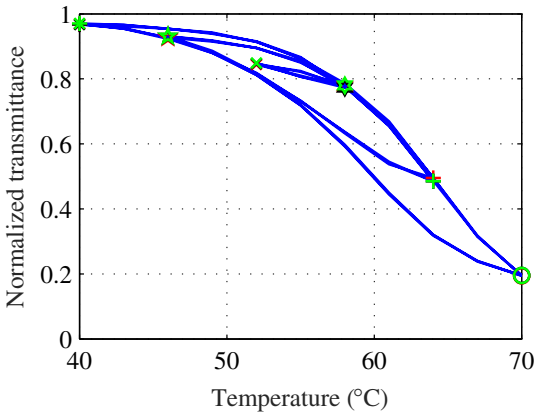

Fig. 8. Transmittance versus temperature curve for validation of the wiping-out property.

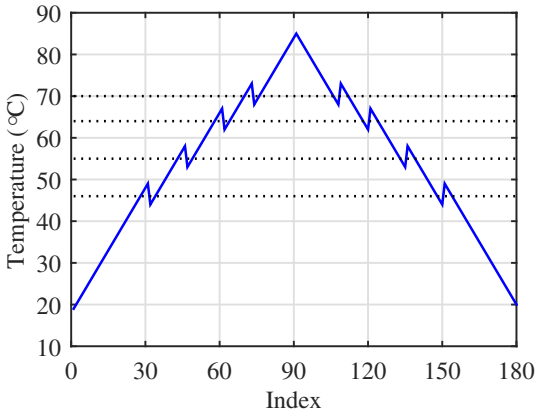

Fig. 9. Temperature profile for congruency property validation.

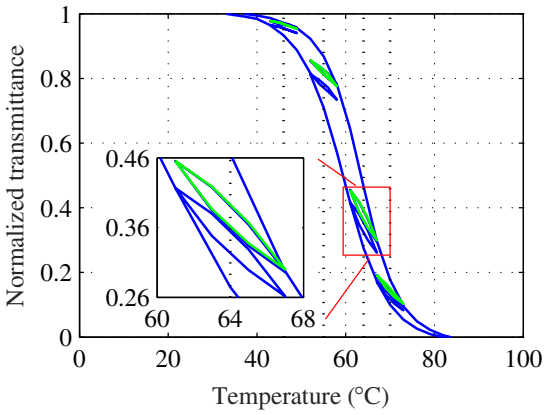

Fig. 10. Transmittance versus temperature curve (vertically shifted minor loop shown in green).

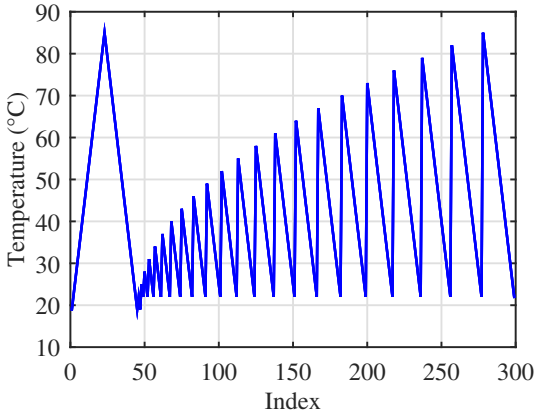

Fig. 11. Temperature profile for identifying the Preisach weights.

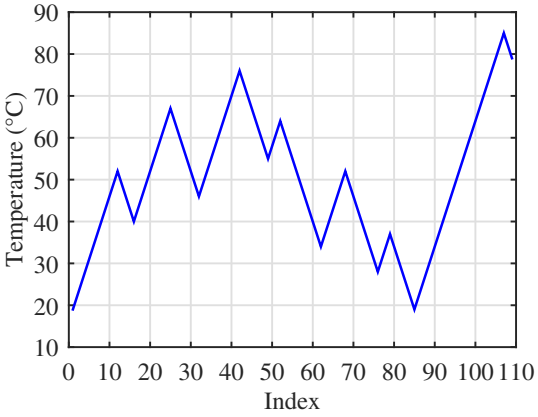

Fig. 12. Temperature profile for model validation.

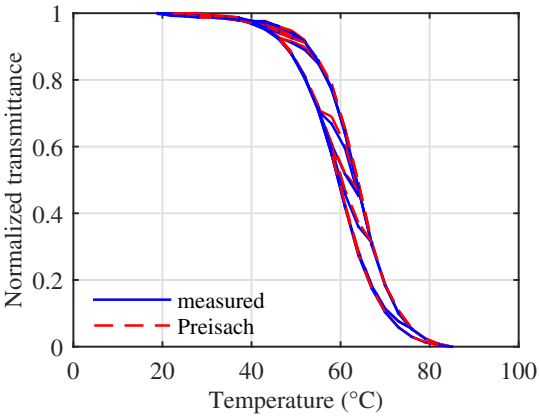

Fig. 13. Model validation for Preisach model.

IV. Relationship between Optical and Electrical Properties

In contrast to the optical behavior, the electrical conductance of a planar binary resistor network exhibits much more complex behavior. Isolated conductive elements embedded in an insulating matrix do not change the conductance at all. Rather, the conductance is dominated by the insulating phase, until a critical area fraction called the "percolation threshold" is reached. At that point the conductance will rise according to a power law, until the overall film behavior becomes dominated by the conductive phase [18]-[19]. That is, the relationship between the conductance and the fraction

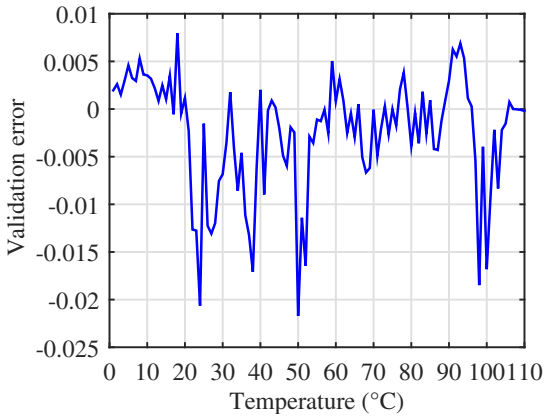

Fig. 14. Validation error for Preisach model.

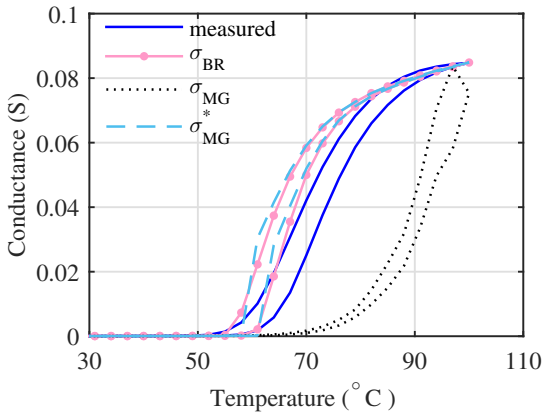

Fig. 15. Comparison of Bruggeman, Maxwell-Garnett, and adapted Maxwell-Garnett EMA conductance models.

of transformed material is not linear, and hence it is not expected that the Preisach model will hold. Therefore it is our claim in this paper that the fundamental material behavior should be described using optical measurements, and electrical conductance can be derived from that, using effective medium approximation (EMA), percolation model, or related approach [18], [20], [21]. We investigate approaches based on EMA and percolation model in this paper.

A. *Effective Medium Approximation*

The EMA is used to describe properties of composite materials. In the EMA setting, the effective conductance of a VO_2 film can be described as inclusion of metallic particles in a matrix of nonmetallic particles. As the temperature rises, nonmetallic particles transform to the metallic phase. We investigate the Bruggeman and Maxwell-Garnett formulations of EMA, described by the following formulas:

$$\sigma_{BR} = \frac{1}{4}\{\sigma_s(2-3f_m)+\sigma_m(3f_m-1) + \sqrt{[\sigma_s(2-3f_m)+\sigma_m(3f_m-1)]^2+8\sigma_s\sigma_m}\} \quad (3)$$

$$\sigma_{MG} = \sigma_s \frac{\sigma_m(1+2f_m)-\sigma_s(2f_m-2)}{\sigma_s(2+f_m)+\sigma_m(1-f_m)} \quad (4)$$

where f_m is the metallic fraction that can be derived from transmittance data; temperature-dependent functions for conductance of non-metallic and metallic phases are denoted by $\sigma_s(T)$ and $\sigma_m(T)$ respectively (with (T) omitted for the purpose of simplicity).

The Drude model [22] describes and formulates temperature-dependent conductance of metal. From the Drude model we can formulate the temperature-dependent conductance of VO_2 in metallic σ_m and nonmetallic σ_s phase as,

$$\sigma_s = m_1 \frac{1}{T+273.15} + c_1 \quad (5)$$

$$\sigma_m = \exp(m_2 \frac{1}{T+273.15} + c_2) \quad (6)$$

where m_1, m_2, c_1 and c_2 can be identified from the measured data.

Fig. 15 shows conductance results for the Bruggeman and the Maxwell-Garnett models. From Fig. 15, we observe that both formulations show significant deviation from the measured data. The Bruggeman formulation assumes that all the inclusions are located in an equivalent mean field. However near the percolation threshold, the conductance of the system is governed by the largest cluster of metallic domain. These correlations are absent in Bruggeman formulation. On the other hand, the Maxwell-Garnett model assumes that the domains are spatially separated and so it is expected to be valid only for low metallic fraction. Likewise the Maxwell-Garnett formulation can be written in terms of the nonmetallic clusters, and should be valid for high metallic fraction. Combining these yields the following adapted Maxwell-Garnett model:

$$\sigma^*_{MG} = \begin{cases} \sigma_s \frac{\sigma_m(1+2f_m)-\sigma_s(2f_m-2)}{\sigma_s(2+f_m)+\sigma_m(1-f_m)} & f_m \le 50\% \\ \sigma_m \frac{\sigma_s(1+2f_s)-\sigma_s(2f_s-2)}{\sigma_m(2+f_s)+\sigma_s(1-f_s)} & f_m > 50\% \end{cases} \quad (7)$$

where f_s = 1 - f_m. Again, this result does not describe the data well.

B. *Percolation Model of Conductance*

We now consider percolation models for the electrical properties. It is reported in the literature [21] that, for material near percolation threshold f_c, the conductance σ has the form

$$\sigma \propto (f_m - f_c)^\zeta \theta(f_m - f_c) \quad (8)$$

where θ is the Heaviside step function. The conductance exponent ζ is well-established to be about 1.3 for the 2D case. We adapt this formulation to describe the conductance of VO_2 as,

$$\sigma[T] = \begin{cases} \sigma_s & f_m < f_c \\ a(T)(f_m - f_c)^\zeta + b(T) & f_c \le f_m \le 1 \end{cases} \quad (9)$$

It is clear that the conductance of the VO_2 material should be σ_s for $f_m \le f_c$, and σ_m for f_m = 1. For continuity, $a(T)$

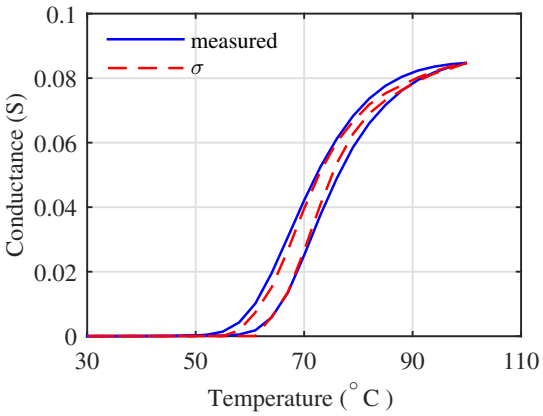

Fig. 16. Estimation of conductance with percolation model (9).

and $b(T)$ can be chosen in the following forms

$$a(T) = \frac{\sigma_m - \sigma_s}{(1-f_c)^{1/\zeta}} \left(\frac{1-f_m}{1-f_c}\right)^{\gamma} \tag{10}$$

$$b(T) = \frac{\sigma_m - \sigma_s}{(1-f_c)^{1/\zeta}} \left(\frac{f_m - f_c}{1-f_c}\right)^{\gamma} (f_m - f_c)^{1/\zeta} + \sigma_s \tag{11}$$

where γ is a tuning parameter. Setting γ = 2.2, f_c = 0.35 and ζ = 1.3, we obtain the conductance estimate shown in Fig. 16. This model shows better agreement with the experiments than the EMA methods. Based on these results, the percolation model seems to be the most promising approach to modeling conductance in VO_2 thin films.

V. Conclusion & Future Work

Simultaneous electrical and optical measurements on thin VO_2 films shows that, unlike the electrical behavior, optical transmissivity versus temperature hysteresis is accurately modeled using a standard Preisach model. Rather than fit independent models to the electrical characteristic, we explore the use of effective medium and percolation models to predict the electrical properties directly from the fraction of material transformed. The results suggest that percolation models hold the most promise. Further refinement of the percolation model is a topic of current work, as is accommodating temperature dependence in the low- and high-temperature phases. Also of current interest is developing similar approaches for properties such as mechanical strain.

References

[1] M. B. Sahana, G. N. Subbanna and S. A. Shivashankar, "Phase transformation and semiconductor-metal transition in thin films of VO_2 deposited by low-pressure metalorganic chemical vapor deposition," *Journal of Applied Physics*, vol. 92, no. 11, pp. 6495–6504, 2002.

[2] W. R. Roach and I. Balberg, "Optical induction and detection of fast phase transition in VO_2," *Solid State Communications*, vol. 9, no. 9, pp. 551–555, 1971.

[3] F. Cardillo Case, "Modifications in the phase transition properties of predeposited VO_2 films," *Journal of Vacuum Science and Technology A*, vol. 2, no. 4, pp. 1509–1512, 1984.

[4] R. Lopez, T. E. Haynes, L. A. Boatner, L. C. Feldman and R. F. Haglund, "Size effects in the structural phase transition of VO_2 nanoparticles," *Physical Review B*, vol. 65, no. 22, pp. 224113, 2002.

[5] C. Chen, X. Yi, J. Zhang and B. Xiong, "Micromachined uncooled IR bolometer linear array using VO_2 thin films," *International Journal of Infrared and Millimeter Waves*, vol. 22, no. 1, pp. 53–58, 2001.

[6] J. Zhang, E. Merced, N. Sepulveda and X. Tan, "Modeling and inverse compensation of nonmonotonic hysteresis in VO_2-coated microactuators," *IEEE/ASME Transactions on Mechatronics*, vol. 19, no. 2, pp. 579–588, 2014.

[7] L. Jiang and W. N. Carr, Design, "Fabrication and testing of a micromachined thermo-optical light modulator based on a vanadium dioxide array," *Journal of Micromechanics and Microengineering*, vol. 14, no. 7, pp. 833–840, 2004.

[8] F. Dumas-Bouchiat, C. Champeaux, A. Catherinot, A. Crunteanu and P. Blondy, "RF-microwave switches based on reversible semiconductor-metal transition of VO_2 thin films synthesized by pulsed-laser deposition," *Applied Physics Letters*, vol. 91, p. 223505, 2007.

[9] J. Zhang, D. Torres, E. Merced, N. Seplveda, and X. Tan, "A hysteresis-compensated self-sensing scheme for vanadium dioxide-coated microactuators," in *ASME Dynamic Systems and Control Conference*, p. V003T45A006, 2014.

[10] J. Zhang, E. Merced, N. Seplveda, and X. Tan, "Modeling and inverse compensation of hysteresis in vanadium dioxide using an extended generalized Prandtl-Ishlinskii model," *Smart Materials and Structures*, vol. 23, no. 12, p. 125017, 2014.

[11] I. D. Mayergoyz, *Mathematical Models of Hysteresis*. Springer-Verlag, 1991.

[12] A. Visintin, *Differential Models of Hysteresis*. Springer-Verlag, 1994.

[13] R. Dong and Y. Tan, "A modified Prandtl-Ishlinskii modeling method for hysteresis," *Physica B: Condensed Matter*, vol. 404, no. 8, pp. 1336–1342, 2009.

[14] M. Ismail, F. Ikhouane, J. Rodellar, "The hysteresis Bouc-Wen model, a survey," *Archives of Computational Methods in Engineering*, vol. 16, no. 2, pp. 161–188, 2009.

[15] L. A. L. de Almeida, G. S. Deep, A. M. N. Lima and H. F. Neff, "Modeling of the hysteretic metal-insulator transition in a vanadium dioxide infrared detector," *Optical Engineering*, vol. 41, no. 10, pp. 2582–2588, 2002.

[16] L. A. L. de Almeida, G. S. Deep, A. M. N. Lima, H. F. Neff, and R. C. S. Freire, "A hysteresis model for a vanadium dioxide transition-edge microbolometer," *IEEE Transactions on Instrumentation and Measurement*, vol. 50, no. 4, pp. 1030–1035, 2001.

[17] L. J. van der Pauw, "A Method of Measuring the Resistivity and Hall Coefficient on Lamellae of Arbitrary Shape," *Phillips Technical Review*, Vol. 20, pp. 220–224, 1958/59.

[18] S. Kirkpatrick, "Percolation and conduction," *Reviews of Modern Physics*, vol. 45, no. 4, pp. 574–588, 1973.

[19] J. Rozen, R. Lopez, R. F. Haglund, Jr., and L. C. Feldman, "Two-dimensional current percolation in nanocrystalline vanadium dioxide films," *Applied Physics Letters*, vol. 88, p. 081902, 2006.

[20] P. U. Jepsen, B. M. Fischer, A. Thoman, H. Helm, J. Y. Suh, R. Lopez, and R. F. Haglund, Jr. "Metal-insulator phase transition in a VO_2 thin film observed with terahertz spectroscopy," *Physical Review B*, vol. 74, no. 20, p. 205103, 2006.

[21] M. B. Isichenko, "Percolation, statistical topography, and transport in random media," *Reviews of Modern Physics*, vol. 64, no. 4, pp. 961–1043, 1992.

[22] C. F. Bohren and D. R. Huffman, *Absorption and Scattering of Light by Small Particles*. John Wiley & Sons, 2008.